

Cytochrome c Peroxidase from *Phanerochaete chrysosporium*

Nonaka, Daisuke

Laboratory of Bioresources Chemistry, Division of Biomaterial Sciences, Department of Forest and Forest Products Sciences, Graduate School of Bioresource and Bioenvironmental Sciences, Kyushu University

Wariishi, Hiroyuki

<https://doi.org/10.5109/4633>

出版情報 : 九州大学大学院農学研究院紀要. 50 (1), pp.151-164, 2005-02-01. Faculty of Agriculture, Kyushu University

バージョン :

権利関係 :

Cytochrome *c* Peroxidase from *Phanerochaete chrysosporium*

Daisuke NONAKA¹ and Hiroyuki WARIISHI*

Laboratory of Bioresources Chemistry, Division of Biomaterial Science, Department of
Forest and Forest Products Sciences, Faculty of Agriculture,
Kyushu University, Fukuoka 812–8581, Japan

(Received November 5, 2004 and accepted November 15, 2004)

Cytochrome *c* peroxidase from the white-rot basidiomycete *Phanerochaete chrysosporium* (PcCcP) was investigated. A phylogenetic analysis of PcCcP amino acid sequence showed that PcCcP was closely related to cytochrome *c* peroxidase from *Saccharomyces cerevisiae* (yeastCcP) and pea cytosolic ascorbate peroxidase (APX). Recombinant PcCcP was obtained by expression in *Escherichia coli* and a heme incorporation into the apoenzymes. Spectral characteristics indicated that the heme iron of PcCcP was mainly 5-coordinated high spin species. The absorption spectrum of PcCcP compound I and rapid-scan spectra of compound I formation strongly suggested that PcCcP compound I was ferrioxo heme iron and protein cation radical, as observed in yeastCcP. Although several typical peroxidase substrates, small organic or inorganic compounds, were not oxidized by PcCcP, ferrocyclochrome *c* was effectively oxidized. Both PcCcP and yeastCcP shared catalytic features. A homology modeling of PcCcP and cytochrome *c* from *P. chrysosporium* (PcCc) strongly suggested the interaction between PcCcP and PcCc.

INTRODUCTION

Lignin is a heterogeneous, phenylpropanoid polymer that constitutes 20–30% of woody plant cell walls (Sarkanen *et al.*, 1970). White-rot basidiomycetous fungi are primarily responsible for initiating the depolymerization of lignin, which is a key step in the earth's carbon cycle (Crawford, 1980; Gold *et al.*, 1989; Kirk and Farrell, 1987; Tien, 1987). The best-studied lignin-degrading fungus, *Phanerochaete chrysosporium*, secretes two types of extracellular heme peroxidases, lignin peroxidase (LiP) and manganese peroxidase (MnP), which are the major extracellular components of its lignin degradative system (Gold *et al.*, 1989; and Kirk and Farrell, 1987). Both enzymes were known to catalyze the first step of degradation of lignin polymers using hydrogen peroxide (Gold *et al.*, 1989).

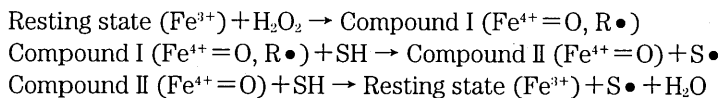
Since the whole genomic sequence of *P. chrysosporium* was made open to public (Martinez *et al.*, 2004), the survey for all heme peroxidase genes in the *P. chrysosporium* genome via BLAST homology search was performed. Several LiP and MnP gene fragments as well as a gene fragments showing a high similarity to cytochrome *c* peroxidase from *Saccharomyces cerevisiae* (yeastCcP) were found.

YeastCcP (ferrocyclochrome *c*/hydrogen peroxide oxidoreductase; EC 1.11.1.5) occurs naturally in the mitochondrial intermembrane space and catalyzes the H₂O₂-dependent

¹ Laboratory of Bioresources Chemistry, Division of Biomaterial Sciences, Department of Forest and Forest Products Sciences, Graduate School of Bioresource and Bioenvironmental Sciences, Kyushu University

* Corresponding author (E-mail: hirowari@agr.kyushu-u.ac.jp)

one-electron oxidation of ferrous cytochrome *c* (Cc^{2+}) to ferric cytochrome *c* (Cc^{3+}) (Bosshad *et al.*, 1990). Most striking difference between yeastCcP and common peroxidases are found in their compound I structures (Sivaraja *et al.*, 1989; Erman and Yonetani, 1975). Generally, a peroxidase catalytic cycle was described as below.



In the first step of the peroxidase catalytic cycle, the resting state enzyme, which has ferric heme iron, is oxidized by hydrogen peroxide to form compound I, where R is an organic moiety. Then, compound I is reduced back to the resting enzyme via compound II by subtracting two electrons from reducing substrates (SH). Usually, peroxidase compound I was comprised of ferryl-oxo heme iron and porphyrin π cation radical. In yeastCcP compound I, ferryl-oxo heme iron is also formed as observed in most other peroxidases; however, cation radical is located at Trp191 rather than porphyrin π cation radical (Sivaraja *et al.*, 1989). In addition, interaction and electron transfer between yeastCcP and cytochrome *c* have been well studied as a model system for two macromolecules (Bosshard *et al.*, 1990; Erman and Vitello, 2002).

Consequently, yeastCcP has been paid much attention in respect to those unique functions and catalytic mechanisms. Since the forefront research techniques have been applied to yeastCcP to reveal its characters, yeastCcP became the paradigm for all other peroxidases.

In the present study, a structural characterization of cytochrome *c* peroxidase (PcCcP) gene from *P. chrysosporium* as well as its cloning and heterologous expression in *Escherichia coli* is reported. The recombinant protein exhibited the H_2O_2 -dependent activity of ferrous cytochrome *c* oxidation.

MATERIALS AND METHODS

Chemicals

H_2O_2 (30% solution) and 2, 6-dimethoxyphenol (DMP) were obtained from Wako Pure Chemicals Co. Ltd. H_2O_2 stock solution (10 mM) was prepared daily and the concentration was checked as previously described (Cotton and Dunford, 1973). DMP was recrystallized from ethanol/hexane. All other chemicals were of reagent grade. Deionized water was obtained from Milli Q system (Millipore).

Cloning of PcCcP gene and construction of the expression vector

P. chrysosporium cDNA was synthesized from totalRNA, which was isolated from 4-day-old stationary culture of *P. chrysosporium*, with M-MLV reverse transcriptase (Takara) and oligo dT primers. Following primers were constructed according to BLAST results using yeastCcP amino acid sequence against *P. chrysosporium* genome sequence; CcP-S-51 (AGGGCTGCGGGCCTCCGTAA, 20 mer), CcP-A-1448 (CGTATATGAGCATCTATGACGCCTCGCA, 28 mer). PcCcP fragment was synthesized by polymerase chain reaction, using CcP-S-51 and CcP-A-1448, and cloned into pGEM-T Easy Vector

(Promega). Signal peptide prediction was achieved using SOSUI (<http://sosui.proteome.bio.tuat.ac.jp/sosui/frame0E.html>) and SignalP (<http://www.cbs.dtu.dk/services/SignalP-2.0/>) programs. For expression of PcCcP polypeptides in *E. coli*, a mature PcCcP sequence with 74 base pairs truncated fragment was amplified using following primers; PcCcP_exp_forw (CCCAAGCTTCATATGAGCGAAGCCGCGAAATCTG; 34mer) and PcCcP_exp_reve (CGGGATCCCTACGACGACTTCGCCTCCT; 28mer). The resulting fragment was digested with Nde I and Bam HI and cloned into pET-12a (+) (Novagen). Resulting vector was named pET-tPcCcP.

Expression of PcCcP in *Escherichia coli*

E. coli BL21(DE3)pLysS (Novagen) transformed with pET-tPcCcP was grown in LB-broth supplemented with 100 µg/ml ampicillin and 34 µg/ml chloramphenicol at 37°C. An initial small-scale expression was conducted in 2 ml culture at 30°C or 37°C. At the time of O.D.₆₀₀ showing ~0.6, 0.4 mM isopropyl-thio-β-D-galactopyranoside (IPTG), 0.5 mM 5-aminolevulinic acid (ALA), and 0.2 mM ferrous sulfate was added to induce the expression of active PcCcP. Incubation time was prolonged for another 6 to 21 h. The cells were harvested by centrifugation at 9,000 rpm for 3 min and directly used for activity assay.

Purification of PcCcP

For a larger-scale preparation of PcCcP, the cells were grown in a 3-L jar-fermenter without the addition of ALA and ferrous sulfate; thus, apo-PcCcP was obtained. After collection of the cells by centrifugation, they were resuspended in 50 mM Tris-Cl, pH 8.0 containing 2 mM EDTA and stored at -80°C. Then, 2 mg/ml lysozyme, 1 mM phenyl-methylsulfonylfluoride, 0.1% Triton X-100, 1 U DNase, and 1 U RNase were added and incubated for 1 h at 30°C with gentle stirring. The incorporation of heme into apo-protein was achieved as reported for the yeastCcP expression system (Teske *et al.*, 2000). A concentrated hemin solution (final concentration of ~500 µM) was added into the lysed cell suspension and incubated at 4°C for at least 30 min with gentle stirring. Then, the solution was acidified at pH 5.0 with 1 M acetic acid, and incubated on ice for 30 min. During this procedure, a large amount of contaminated proteins and excess heme were precipitated. After centrifugation, the solution was diluted by 20 times with deionized water and pH of the solution was adjusted to pH 6.0. The enzyme solution was loaded onto DEAE Sepharose Fast Flow (Amersham Biosciences) equilibrated with 10 mM phosphate, pH 6.0. PcCcP was eluted with 500 mM phosphate, pH 6.0. The fractions showing CcP activity were combined and dialysed against 10 mM phosphate, pH 6.0, for 16 h. The dialyzed sample was concentrated and final purification was achieved using Mono-Q (Amersham Biosciences) with a multilinear gradient with 10 mM phosphate, pH 6.0 and 1 M phosphate, pH 6.0 at a flow rate of 1 ml/min. The purified enzyme was dialyzed against deionized water overnight and stored at 4°C.

Cytochrome *c* preparations

Yeast iso-1 cytochrome *c* were purchased from Aldrich and used without further purification. Ferrous cytochrome *c* (Cc²⁺) was prepared as previously described (Johjima *et al.*, 2002; Wariishi *et al.*, 1994). Concentration of Cc²⁺ was determined spectrophoto-

tometrically using a molar extinction coefficient at 550 nm of $27.6 \text{ mM}^{-1} \text{ cm}^{-1}$ (Yonetani, 1965).

Spectroscopic Analysis

Electronic absorption spectra were recorded using a Perkin Elmer Lambda 19 spectrophotometer at 25 °C.

Steady-state kinetic analysis

Initial rates of substrate oxidation were spectrophotometrically measured at 25 °C. All steady-state kinetic experiments were performed in 20 mM phosphate, pH 6.0. The rate of DMP oxidation (quinone dimmer formation) was determined from the increase in absorbance at 469 nm using $\Delta\epsilon$ of $49.6 \text{ mM}^{-1} \text{ cm}^{-1}$ (Wariishi *et al.*, 1992). The rate of ferrocyanide oxidation (ferricyanide formation) was determined using $\Delta\epsilon_{420}$ of $1.02 \text{ mM}^{-1} \text{ cm}^{-1}$ (Schellenberg and Hellerman., 1958). The rate of ABTS oxidation (ABTS cation radical formation) was determined using $\Delta\epsilon_{415}$ of $36.0 \text{ mM}^{-1} \text{ cm}^{-1}$ (Smith *et al.*, 1990). All reactions were initiated by adding 0.1 mM H_2O_2 . Steady-state kinetic parameters were calculated from the Lineweaver-Burk plot. The reaction of PcCcP with Cc^{2+} and L-ascorbate was determined at 550 nm and 290 nm, respectively.

Transient-state kinetic analysis

Kinetic measurements were conducted using a Photol RA 401S Rapid Reaction Analyzer (Otsuka Electronics Co. Ltd.) equipped with a 1-cm observation cell at 25.0 ± 0.1 °C. The formation rate of PcCcP compound I was determined at 417 nm, the maximum absorption wavelength of compound I. One reservoir contained native PcCcP (ca. $2 \mu\text{M}$) and the other reservoir contained H_2O_2 (5–15 μM) in 40 mM phosphate, pH 6.0. The pseudo-first order rate constants were determined by a non-linear least-squares fit to exponential traces.

Homology modeling of PcCcP

A homology model of the PcCcP tertiary structure was constructed with MOE program (Chemical Computing Group Inc.), according to manufacturer's instructions and as previously reported (Rupasinghe *et al.*, 2003), using yeastCcP structure (PDB code: 2CYP) as a template structure. The truncated PcCcP amino acid sequence with a deletion of 82 amino acids in N-terminal and 10 amino acids in C-terminal sequences from the original sequence was applied to homology model programs, since those sequences showed no homology to the mature yeastCcP sequence. After construction of the initial homology model, further energy minimization was performed using the CHARMM22 force field (MacKerell *et al.*, 1998) within the MOE distribution until the final energy gradient became $< 0.01 \text{ kcal/mol. \AA}$. A distance-dependent dielectric constant was used in the calculations with a cutoff between 6.5 and 7 \AA .

RESULTS AND DISCUSSION

PcCcP amino acid sequence

The fragment showed a high similarity to the yeastCcP sequence was amplified using

primers designed from the *P. chrysosporium* genome sequence (Martinez *et al.*, 2004). The resulting fragment was cloned and sequenced. A phylogenetic analysis of the deduced PcCcP amino acid sequence and several typical peroxidases clearly showed that PcCcP was classified into class I plant peroxidase superfamily, which was comprised of intracellular peroxidases from plant and bacteria, and that the most closely related to yeastCcP (43%) and pea cytosolic ascorbate peroxidase (APX) (41%) (Fig. 1).

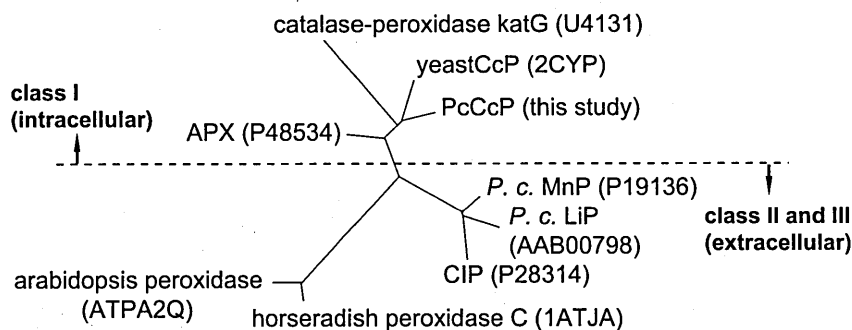


Fig. 1. Phylogenetic tree of PcCcP and typical peroxidases. Phylogenetic tree was calculated and visualized by Tree View program using Neighbor-Joining method (Saitou *et al.*, 1987). NCBI accession numbers of each protein were shown in parenthesis.

A further detailed analysis of the PcCcP amino acid sequence was performed via ClustalW alignment using yeastCcP and APX (Fig. 2). Essential amino acids for peroxidative mechanism, e.g. the proximal histidine, distal histidine, and distal arginine, were also conserved in PcCcP. One of the most interesting characteristics of yeastCcP was its compound I structure. YeastCcP compound I has been known to possess ferryl-oxo heme iron and Trp191 cation radical rather than ferryl-oxo heme iron and porphyrin π cation radical found in plant and fungal peroxidases (Sivaraja *et al.*, 1989). Sequential analysis revealed that the existence of Trp residue (Trp275) in PcCcP at the corresponding position of Trp191 in yeastCcP. Furthermore, yeastCcP is known to oxidize Cc^{2+} , its physiological substrate, on the protein surface (Bosshard *et al.*, 1990). Because of basic character of Cc^{2+} , yeastCcP was known to possess acidic amino acid residues involved in Cc^{2+} binding on its protein surface (Pelletier and Kraut, 1992 and Guo *et al.*, 2004). Sequential alignment analysis revealed that PcCcP has such acidic residues, which might construct a Cc^{2+} binding site on the surface of PcCcP. Interestingly, amino acid residues forming a proposed electron transfer pathway W¹⁹¹G¹⁹²A¹⁹³A¹⁹⁴ in yeastCcP (Pelletier and Kraut, 1992), was replaced in PcCcP as W²⁷⁵T²⁷⁶F²⁷⁷S²⁷⁸.

A PSORT analysis of PcCcP amino acid sequence suggested that PcCcP might localize in mitochondria and first 65 amino acids from initial methionine might be a signal peptide. Furthermore, SOSUI program suggested that PcCcP has a transmembrane region (Fig. 2, underlined) in its N-terminal. PcCcP might be localized in mitochondria as shown for yeastCcP.

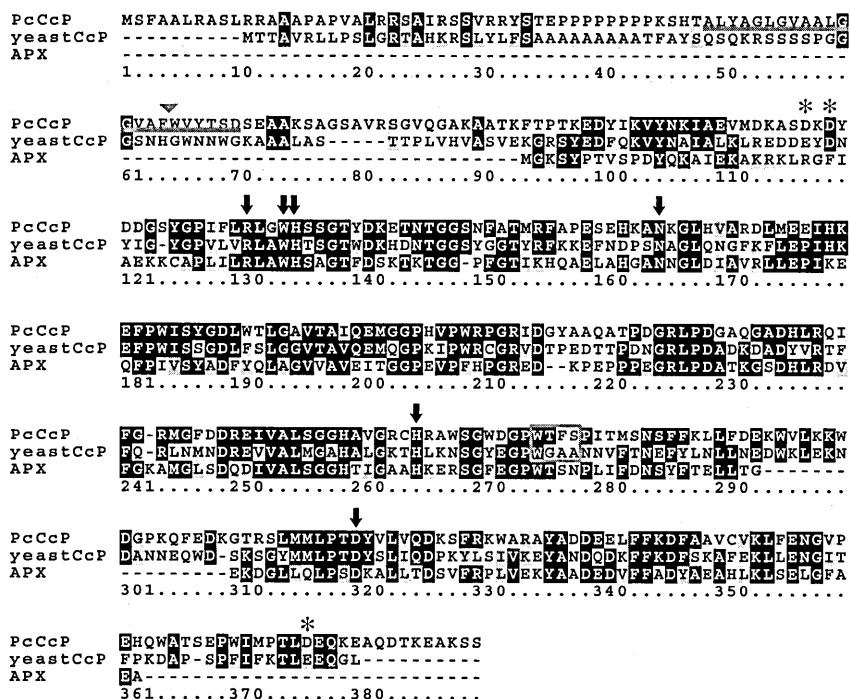


Fig. 2. ClustalW alignment of amino acid sequences between PcCcP, yeastCcP and APX. The alignment was generated by ClustalW and visualized by boxshade program. Arrows indicate conserved amino acids, which are essential for peroxidative activity. Amino acids involved in electron transfer between yeastCcP and Cc^{2+} were enclosed in a gray box. Acidic amino acids, involved in binding of basic Cc^{2+} at the enzyme surface of yeastCcP, are indicated in asterisks. Underlined residues at N-terminal are membrane-bound region predicted by SOSUI program and a triangle indicates the signal peptides cleavage site which was predicted by PSORT program.

Expression of PcCcP in *E. coli*

According to PSORT and SOSUI results, the first 71 amino acids were truncated and designed to have N-terminal sequence of MSEAA-, then cloned into pET-12a(+). *E. coli* strain BL21(DE3)pLysS transformed with pET-tPcCcP was grown in LB culture containing ALA and $FeSO_4$. Six hours after induction, cells were collected and the H_2O_2 -dependent Cc^{2+} oxidation activity of the lysed cells was determined (Fig. 3). Only when Cc^{2+} was incubated with the induced cells and hydrogen peroxide, Cc^{2+} oxidation activity was observed. The highest activity was observed after a 14-h incubation at 30°C (data not shown). Fig. 4 illustrated SDS-PAGE analysis of expression of PcCcP in *E. coli* strain BL21(DE3)pLysS. PcCcP polypeptides were expressed only in IPTG induced cells. The predicted molecular weight of 33.6 kDa was confirmed for expressed PcCcP. Incubation at 37°C resulted in accumulation of insoluble form of PcCcP polypeptides as inclusion bodies.

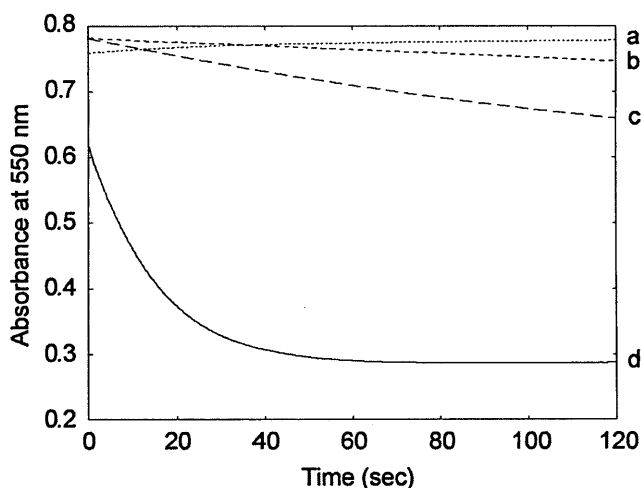


Fig. 3. Ferrocyanide oxidation by PcCcP expressed in *E. coli*. $34\mu\text{M}$ Cc^{2+} was incubated with IPTG-induced *E. coli* cells only (trace a), 0.1 mM H_2O_2 only (trace b), non-induced *E. coli* cells and 0.1 mM H_2O_2 (trace c), and induced *E. coli* cells and 0.1 mM H_2O_2 (trace d) in 20 mM phosphate, pH 7.2.

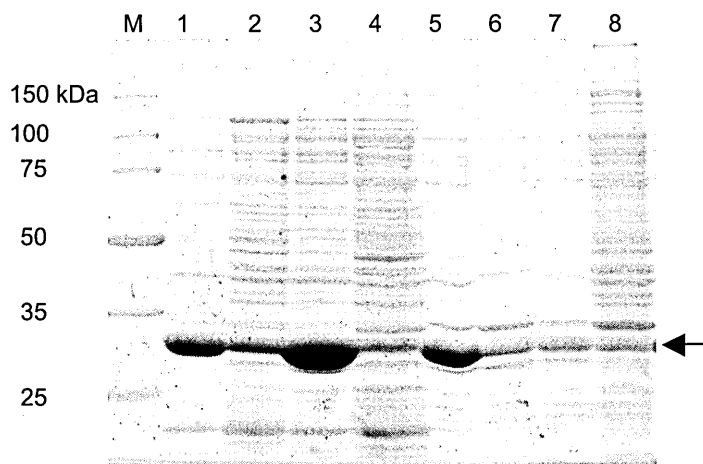


Fig. 4. SDS-PAGE analysis of PcCcP protein expressed in *E. coli*. Expression of PcCcP were induced (lanes 1–3 and 5–7) by the addition of 0.4 mM IPTG or not induced (lanes 4 and 8). *E. coli* cells were incubated at 37°C for 6 hours (lanes 1 and 5) and at 30°C for 6 hours (lanes 3, 4, 7 and 8) or 21 hours (lanes 2 and 6). After lysed with lysozyme treatment, proteins were fractionated by centrifugation into soluble fraction (lanes 1–4) and insoluble fraction (lanes 5–8). Bands derived from PcCcP are marked with arrows. Protein samples were prepared with SDS-PAGE sample buffer, which contains 3 M urea, 2% SDS, 2.5% 2-ME, 75 mM DTT and 10% glycerol.

Preparation of recombinant PcCcP

In large-scale incubation, PcCcP protein was recovered as apo-form. An active enzyme was obtained via *in vitro* incorporation of the heme into the apoprotein. Active PcCcP was effectively purified using two chromatograms, DEAE Sepharose Fast Flow and Mono-Q. Elution profile of PcCcP from Mono-Q was shown in Fig. 5. Final yield of the recombinant PcCcP was about 70 mg/L culture medium.

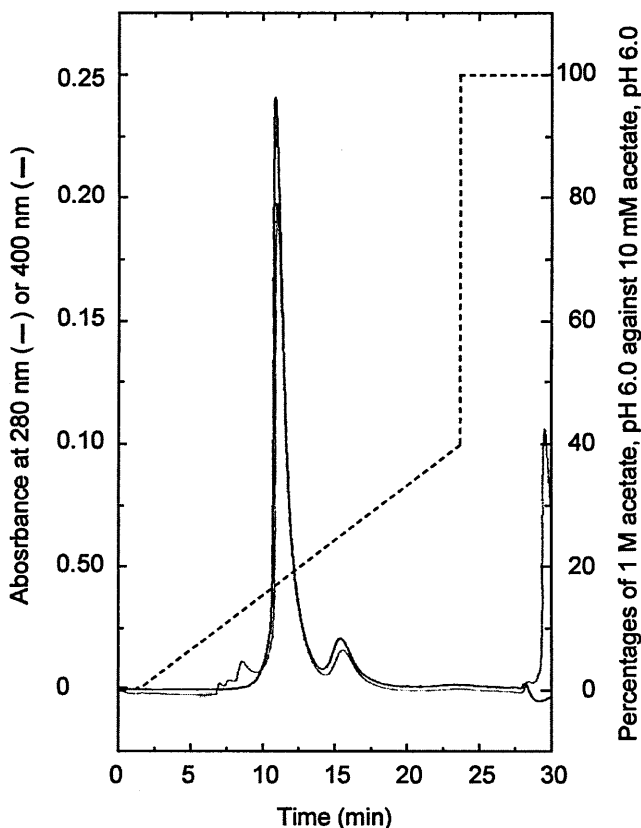


Fig. 5. Elution profile of PcCcP from Mono-Q column. Black and gray lines indicates absorbance at 280 and 400 nm, respectively (on the left y-axis). Dashed line shows percentages of 1 M acetate, pH 6.0 in 10 mM acetate, pH 6.0 (on the right y-axis). PcCcP was eluted at 11.3 min.

Electronic absorption spectra of PcCcP

Purified PcCcP exhibited RZ value of 0.82. Extinction coefficient at 405 nm for the resting enzyme was determined to be $118.9 \text{ mM}^{-1} \text{ cm}^{-1}$ using pyridine-hemochromogen method (Paul *et al.*, 1953). Fig. 6 shows an electronic absorption spectrum of PcCcP in

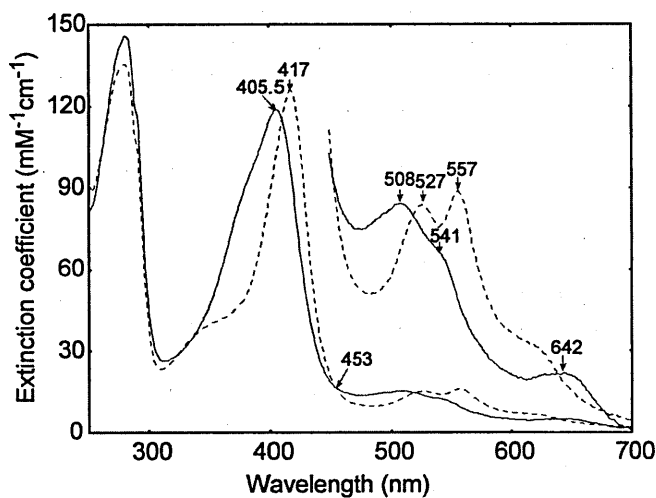


Fig. 6. Electronic absorption spectrum of resting state (solid line) and compound I (broken line). $3\mu\text{M}$ PcCcP was used. Compound I was generated by adding the equimolar hydrogen peroxide to the resting enzyme.

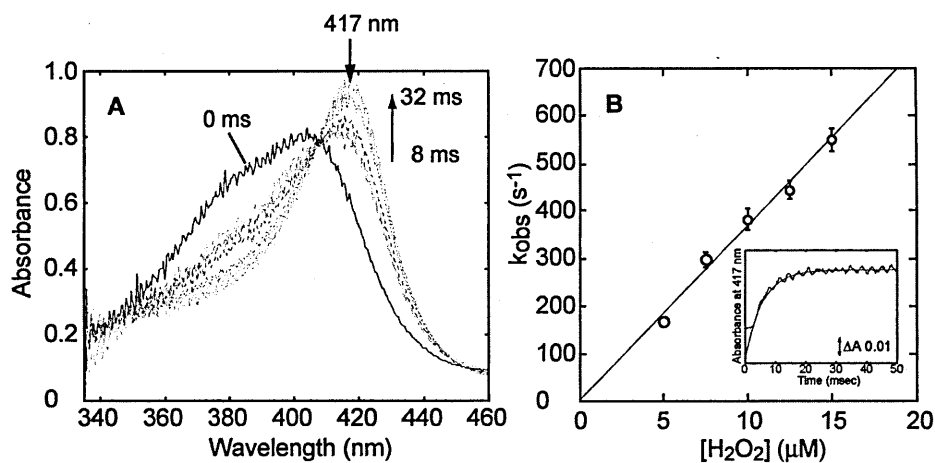


Fig. 7. Transient-state kinetic analysis of PcCcP compound I formation. A: Rapid-scan spectra of compound I formation. B: Compound I formation rate of PcCcP. Inset shows typical kinetic trace at 417 nm.

20 mM phosphate, pH 6.0. The absorption spectrum of resting enzyme showed the Soret maximum at 405.5 nm with a shoulder at ~ 380 nm, and visible peaks at 508 nm, 541 nm and 642 nm, strongly suggesting that the heme iron of recombinant PcCcP was five-coordinated high spin. High numbers of aromatic amino acids (19 phenylalanines, 13 tryptophanes, and 12 tyrosines) in PcCcP is the reason for a low number of RZ value and could also be one of the reasons that easier formation of inclusion bodies, compared to yeastCcP.

PcCcP compound I was generated by adding the equimolar of hydrogen peroxide, resulting in the Soret maximum at 417 nm. The absorption spectrum of PcCcP compound I resembled that of yeastCcP compound I which has the Soret maximum at 419 nm. Thus, PcCcP compound I might contain the ferryl-oxo heme iron and an amino acid cation radical, probably at Trp275.

YeastCcP compound II was reported to be the mixture of ferryl-oxo iron and Trp cation radical; thus, its absorption spectrum is not distinguishable (Coulson *et al.*, 1971). PcCcP compound II was prepared by adding equimolar ferrocyanide to PcCcP compound I. The resulting spectrum of PcCcP was very similar to that of the resting state (data not shown), suggesting PcCcP compound II also possessed yeastCcP-like protein based cation radical, probably with less characteristics of ferryl-oxo feature of the heme.

Stopped-flow analysis of PcCcP compound I formation

Further characterization of PcCcP compound I was conducted using a stopped-flow rapid-scan analysis. Fig. 5A showed rapid-scan spectra of the reaction between the resting state enzyme and H_2O_2 from 8 ms to 32 ms after mixing. The isosbestic points at 345, 407, and 455 nm clearly indicated that the reaction proceeded in a single step. Then, the PcCcP compound I formation rate was determined by following the change in absorbance at 417 nm. The values of k_{obs} were obtained using exponential fit to the kinetic traces (Fig. 5B inset). The first-order rate constant for PcCcP formation (k_1) was evaluated to be $3.6 \times 10^7 \text{ M}^{-1} \text{ s}^{-1}$ by plotting k_{obs} values against H_2O_2 concentrations (Fig. 5B). The intersection of the regression line of the plots at the origin indicated that the reaction between PcCcP and H_2O_2 was irreversible.

Cytochrome *c* oxidation by PcCcP

Since PcCcP amino acid sequence showed a high similarity against both yeastCcP and APX, as shown in Fig. 2, one-electron oxidation ability of purified PcCcP against cytochrome *c* and L-ascorbate, which were physiological substrates for yeastCcP and APX, respectively, were investigated. In the presence of H_2O_2 , PcCcP effectively catalyzed an one-electron oxidation of Cc^{2+} (Fig. 8). On the other hand, no significant change was observed in the reaction between PcCcP and L-ascorbate (Fig. 8). These observations strongly suggested that L-ascorbate is not a substrate of PcCcP but Cc^{2+} is.

Substrate specificity of PcCcP

Steady-state kinetic parameters for reactions between PcCcP and a series of typical peroxidase substrates were determined (Table 1). PcCcP showed low activities against DMP (phenolic substrate), ABTS (typical anionic substrate), ferrocyanide (inorganic substrate). Furthermore, veratryl alcohol and manganese (II), which are physiological sub-

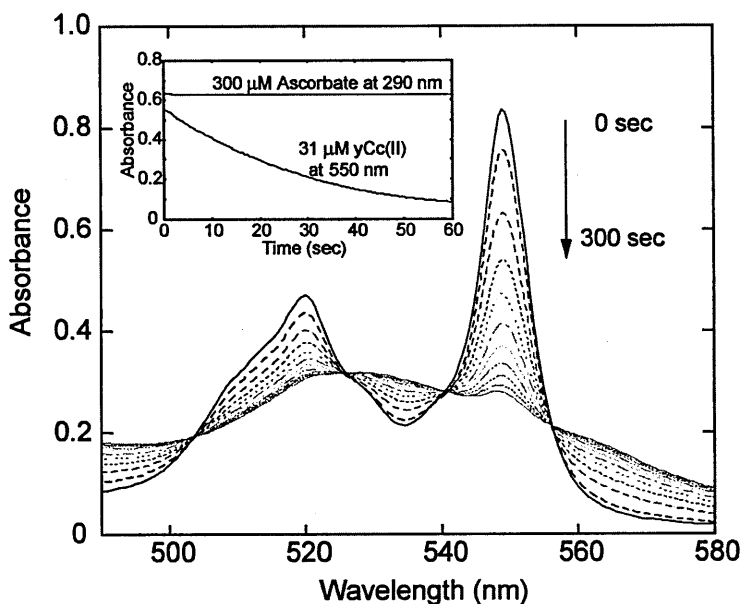


Fig. 8. Time course of the reaction between PcCcP and Cc^{2+} . $31\mu M Cc^{2+}$ was incubated with $0.85 nM$ PcCcP and $50\mu M H_2O_2$ in $20 mM$ phosphate, pH 6.0. Each spectrum was measured every 3 minutes after addition of H_2O_2 . Inset shows kinetic traces of reactions between PcCcP and Cc^{2+} or L-ascorbate.

Table 1. Steady-state kinetic parameters of various substrates oxidation catalyzed by PcCcP.

	K _m (mM)	k _{cat} (mmol/min/mmol)	k _{cat} /K _m (mM ⁻¹ min ⁻¹)
DMP	17	56	3.3
ABTS	0.41	390	951
Ferrocyanide	68	213800	3144

strates for LiP and MnP were not reacted with PcCcP.

Homology modeling of PcCcP

A homology model of PcCcP was constructed with MOE program using yeastCcP crystal structure (2CYP) as a template structure (Fig. 9). Obtained final model showed a root mean square value of 1 \AA against yeastCcP crystal structure (PDB code; 2CYP) in respect to $C\alpha$ carbon, suggesting that the PcCcP structural model was correctly constructed. Pelletier *et al.* (1992) reported that acidic residues on the surface of yeastCcP were involved in binding to basic Cc^{2+} , based on the co-crystal structure of yeastCcP and cytochrome *c*. Acidic amino acids were also existed on the surface of the PcCcP model structure and the number of those residues were much higher than those of yeastCcP,

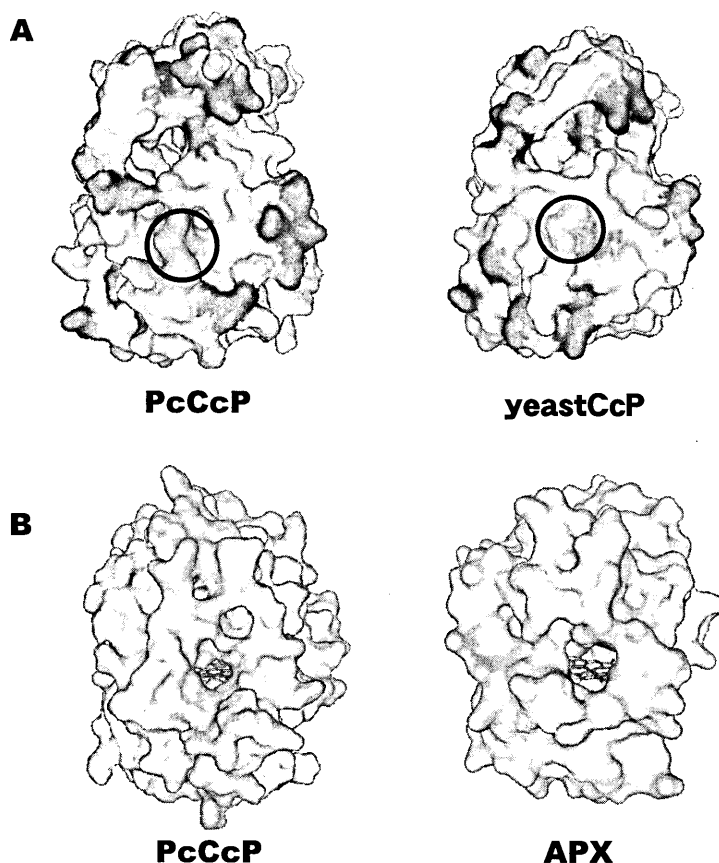


Fig. 9. Homology model of PcCcP. Panel A: Acidic amino acids on the protein surface of PcCcP and yeastCcP. Acidic amino acids (glutamate or aspartate) are indicated in dark color. The proposed electron transfer site in yeastCcP (Pelletier and Kraut, 1992) or the corresponding residues in PcCcP were enclosed in circles. Panel B: Comparison of heme pocket architecture of PcCcP and APX. Heme was emphasized in gray.

indicating surface of PcCcP was much more acidic than that of yeastCcP (Fig. 9A). The model structure for cytochrome *c* of *P. chrysosporium* (PcCc), which was annotated from *P. chrysosporium* genome sequence by a BLAST search using cytochrome *c* sequence of *S. cerevisiae* was constructed. The surface of PcCc was basic with calculated pI of 9.6, which was comparable to pI of 11 for yeast iso-1 cytochrome *c*. Because of lower pI for PcCc, strongly acidic surface characteristics might be required for PcCcP.

APX shows no activity against Cc^{2+} despite of its sequence similarity against yeastCcP. The most preferred substrate of APX is L-ascorbate, its physiological substrate. Crystal structure of ascorbate peroxidase-ascorbate complex (Sharp *et al.*, 2003) showed that cationic amino acid residues, Lys 30 and Arg 172, were mostly contributed to the binding

of L-ascorbate, an anionic substrate. These two cationic amino acids were substituted to Gly and Asn in yeastCcP and Gly and Trp in PcCcP, respectively (Fig. 2). These structural characteristics are in good accordance with the observation that PcCcP exhibited the oxidation activity towards Cc^{2+} but not to L-ascorbate (Fig. 8).

PcCcP showed only a weak activity towards typical peroxidase substrates (Table 1). Furthermore, PcCcP showed no activity against manganese (II) or veratryl alcohol, which were physiological substrates for MnP and LiP, respectively (Gold *et al.*, 1989). These observations clearly indicated that substrate specificity of PcCcP was strictly restricted to Cc^{2+} and, furthermore, PcCcP seemed not to be involved in neither L-ascorbate nor lignin metabolism. Substrate specificity of PcCcP was further evidenced by the homology model of PcCcP. Fig. 9B showed comparison of heme pocket entrance between PcCcP and APX. Narrower heme pocket of PcCcP, compared to that of APX, might prevent the interaction of reducing substrates with the heme of PcCcP.

A physiological function of yeastCcP was not completely understood. Especially, a physiological meaning of Cc^{2+} oxidation by yeastCcP is still unclear. However, the induction of yeastCcP mRNA by oxidative stress was reported (Kwon *et al.*, 2003) and this enzyme might be involved in antioxidant system in mitochondria. Proteomic analysis surveying the conditions to optimize PcCcP production is now underway. Our recent proteomic data indicated the up-regulation of PcCcP production under 100% oxygen atmosphere (data not shown). PcCcP may be involved in antioxidant system.

CONCLUSION

P. chrysosporium genome sequence data enabled us to survey various enzymes. This is the first time to exhibit that cytochrome *c* peroxidase was active and functional in basidiomycetes. Recombinant PcCcP was successfully obtained via the *E. coli* expression system. The structural characteristics were suggested to be very similar to yeastCcP. Spectral, kinetic, and sequential analyses of PcCcP revealed that recombinant PcCcP catalyzes the H_2O_2 -dependent Cc^{2+} oxidation via a typical peroxidase catalytic cycle.

REFERENCES

- Bosshard, H. R., H. Anni and T. Yonetani 1990 Yeast cytochrome *c* peroxidase. In "Peroxidases in Chemistry and Biology" (Everse, J., Everse, K. E., and Grisham, M. B., Eds.), Vol. II, CRC Press, Boca Raton, FL, pp. 51-84
- Cotton, M. L. and H. B. Dunford 1973 Studies on horseradish peroxidase XI: On the nature of compounds I and II as determined from the kinetics of the oxidation of ferrocyanide. *Can. J. Chem.*, **51**: 582-587
- Coulson, A. F. W., J. E. Erman and T. Yonetani 1971 Studies on cytochrome *c* peroxidase. XVII. Stoichiometry and mechanism of the reaction of compound ES with donors. *J. Biol. Chem.*, **246**: 917-924
- Crawford, R. L. 1980 *Lignin Biodegradation and Transformation*, Wiley, New York
- Erman, J. E. and L. B. Vitello 2002 Yeast cytochrome *c* peroxidase: mechanistic studies via protein engineering. *Biochim. Biophys. Acta.*, **1597**: 193-220
- Erman, J. E. and T. Yonetani 1975 A kinetic study of the endogenous reduction of the oxidized sites in the primary cytochrome *c* peroxidase-hydrogen peroxide compound. *Biochim. Biophys. Acta.*, **393**: 350-357
- Gold, M. H., H. Wariishi and K. Valli 1989 Whitaker, J. R. and P. Sonnet (Eds.), *Proceedings of the ACS*

- Symposium Series 389 on Biocatalysis in Agricultural Biotechnology*, American Chemical Society, Washington, DC, pp. 127–140
- Guo, M., B. Bhaskar, H. Li, T. P. Barrows and T. L. Poulos 2004 Crystal structure and characterization of a cytochrome *c* peroxidase–cytochrome *c* site-specific cross-link. *Proc. Natl. Acad. Sci. U. S. A.*, **101**: 5940–5945
- Johjima, T., H. Wariishi and H. Tanaka 2002 Veratryl alcohol binding sites of lignin peroxidase from *Phanerochaete chrysosporium*. *J. Mol. Cat. B: Enzym.*, **17**: 49–57
- Kirk, T. K. and R. L. Farrell 1987 Enzymatic “combustion”: the microbial degradation of lignin. *Annu. Rev. Microbiol.*, **41**: 465–505
- Kwon, M., S. Chong, S. Han and K. Kim 2003 Oxidative stresses elevate the expression of cytochrome *c* peroxidase in *Saccharomyces cerevisiae*. *Biochim. Biophys. Acta.*, **1623**: 1–5
- MacKerell, A. D., Jr., D. Bashford, R. L. Bellott, R. L. Dunbrack, Jr., J. D. Evanseck, M. J. Field, S. Fischer, J. Gao, H. Guo, S. Ha, D. Joseph-McCarthy, L. Kuchnir, K. Kuczera, F. T. K. Lau, C. Mattos, S. Michnick, T. Ngo, D. T. Nguyen, B. Prodhom, W. E. Reiher, III, B. Roux, M. Schlenkrich, J. C. Smith, R. Stote, J. Straub, M. Watanabe, J. Wierkiewicz-Kuczera, D. Yin and M. Karplus 1998 All-Atom Empirical Potential for Molecular Modeling and Dynamics Studies of Proteins. *J. Phys. Chem. B.*, **102**: 3586–3616
- Martinez, D., L. F. Larrondo, N. Putnam, M. D. Gelpke, K. Huang, J. Chapman, K. G. Helfenbein, P. Ramaiya, J. C. Detter, F. Larimer, P. M. Coutinho, B. Henrissat, R. Berka, D. Cullen and D. Rokhsar 2004 Genome sequence of the lignocellulose degrading fungus *Phanerochaete chrysosporium* strain RP78. *Nat. Biotechnol.*, **22**: 695–700
- Paul, K. G., H. Theorell and Å. Åkeson 1953 The molar light absorption of pyridine ferroprotoporphyrin (pyridine haemochromogen). *Acta Chem. Scand.*, **7**: 1284–1287
- Pelletier, H. and J. Kraut 1992 Crystal Structure of a Complex Between Electron Transfer Partners, Cytochrome *c* Peroxidase and Cytochrome *c*. *Science*, **258**: 1748–1755
- Rupasinghe, S., J. Baudry and M. A. Schuler 2003 Common active site architecture and binding strategy of four phenylpropanoid P450s from *Arabidopsis thaliana* as revealed by molecular modeling. *Protein Eng.*, **16**: 721–731
- Saitou, N. and M. Nei 1987 The neighbor-joining method: a new method for reconstructing phylogenetic trees. *Mol. Biol. Evol.*, **4**: 406–425
- Sarkanen, K. V. and C. H. Ludwig 1970 *Lignins: Occurrence, Formation, Structure and Reactions*, Wiley, New York
- Schellenberg, K. A. and L. Hellerman 1958 Oxidation of reduced diphosphopyridine nucleotide. *J. Biol. Chem.*, **231**: 547–556
- Sharp, K. H., M. Mewies, P. C. Moody and E. L. Raven 2003 Crystal structure of the ascorbate peroxidase–ascorbate complex. *Nat. Struct. Biol.*, **4**: 303–307
- Sivaraja, M., D. B. Goodin, M. Smith and B. M. Hoffman 1989 Identification by ENDOR of Trp191 as the free-radical site in cytochrome *c* peroxidase compound ES. *Science*, **245**: 738–740
- Smith, A. T., N. Santama, S. Dacey, M. Edwards, R. C. Bray, R. N. Thorneley and J. F. Burke 1990 Expression of a synthetic gene for horseradish peroxidase C in *Escherichia coli* and folding and activation of the recombinant enzyme with Ca^{2+} and heme. *J. Biol. Chem.*, **265**: 13335–13343
- Teske, J. G., M. I. Savenkova, J. M. Mauro, J. E. Erman and J. D. Satterlee 2000 Yeast cytochrome *c* peroxidase expression in *Escherichia coli* and rapid isolation of various highly pure holoenzymes. *Protein Expr. Purif.*, **19**: 139–147
- Tien, M. 1987 Properties of ligninase from *Phanerochaete chrysosporium* and their possible applications. *CRC Crit. Rev. Microbiol.*, **15**: 141–168
- Wariishi, H., K. Valli and M. H. Gold 1992 Manganese(II) oxidation by manganese peroxidase from the basidiomycete *Phanerochaete chrysosporium*. Kinetic mechanism and role of chelators. *J. Biol. Chem.*, **267**: 23688–23695
- Wariishi, H., D. Sheng and M. H. Gold 1994 Oxidation of ferrocycytochrome *c* by lignin peroxidase. *Biochemistry*, **33**: 5545–5552
- Yonetani, T. 1965 Studies on cytochrome *c* peroxidase. II. Stoichiometry between enzyme, H_2O_2 , and ferrocycytochrome *c* and enzymic determination of extinction coefficients of cytochrome *c*. *J. Biol. Chem.*, **240**: 4509–4514
- Yonetani, T. 1976 *The Enzymes*, 3rd ed., P. D. Boyer, ed., Academic, New York, Vol. 13, pp. 345–361